Chaos synchronization in three coupled SQUIDs

Joniald Shena*

National University of Science and Technology MISiS, Leninsky prosp. 4, Moscow, 119049, Russia

N. Lazarides and J. Hizanidis

Department of Physics, University of Crete, 71003 Heraklion, Greece
(Dated: April 21, 2021)

I. INTRODUCTION

The phenomena of chaos synchronization has also been observed in a system of three coupled lasers [4].

II. THE MODEL

Consider three identical rf SQUIDs in close proximity so that they are coupled by magnetic dipole-dipole forces through their mutual inductance M (Fig. 1). Each of the SQUIDs is modeled by an equivalent electrical circuit that features a self-inductance L due to the superconducting ring, which is connected in series with a "real" Josephson junction characterized by a critical current I_c, capacitance C, and Ohmic resistance R. The SQUIDs are subject to an externally applied spatially constant and time-periodic (ac) magnetic field and a constant in time and space (dc) magnetic field. Those fields add an electromotive force in series to the SQUID's equivalent circuits. The magnetic flux threading the loops of the SQUIDs includes supercurrents as well as normal (i.e., quasiparticle) currents around the SQUID's rings through Faraday's law. In turn, the induced currents produce their own magnetics field which counter-acts the applied ones. Then, the flux Φ_1, Φ_2 and Φ_3 through the loop of the SQUID number 1, 2 and 3, respectively, is given by the following flux-balance relations

$$\Phi_1 = \Phi_{ext} + LI_1 + \mathcal{M}I_2 \tag{1}$$
$$\Phi_2 = \Phi_{ext} + LI_2 + \mathcal{M}(I_1 + I_3) \tag{2}$$
$$\Phi_3 = \Phi_{ext} + LI_3 + \mathcal{M}I_2 \tag{3}$$

where I_1, I_2 and I_3 are the currents induced by the external magnetic fields, and the external flux

$$\Phi_{ext} = \Phi_{dc} + \Phi_{ac}\cos(\omega t) \tag{4}$$

with Φ_{dc} the dc flux bias, Φ_{ac} the amplitude of the ac flux, ω its frequency, and t the temporal variable. Eqs. 1, 2 and 3 can be solved for the currents and written in matrix form as

$$\begin{bmatrix} I_1 \\ I_2 \\ I_3 \end{bmatrix} = \frac{1}{L} \begin{bmatrix} 1 & \lambda & 0 \\ \lambda & 1 & \lambda \\ 0 & \lambda & 1 \end{bmatrix}^{-1} \begin{bmatrix} \Phi_1 - \Phi_{ext} \\ \Phi_2 - \Phi_{ext} \\ \Phi_3 - \Phi_{ext} \end{bmatrix} \tag{5}$$

,

where $\lambda = \frac{\mathcal{M}}{L}$ is the magnetic coupling strength between the SQUIDs. Note that the sign of λ depends on the mutual position of the SQUIDs and in the axial geometry (Fig. 1), it is always positive. The currents flowing in the SQUIDs are given within the framework of the resistively and capacitively shunted junction (RCSJ) model, as

$$I_n = -C\frac{d^2\Phi_n}{dt^2} - \frac{1}{R}\frac{d\Phi_n}{dt} - I_c\sin\left(2\pi\frac{\Phi_n}{\Phi_0}\right) \tag{6}$$

where Φ_0 is the flux quantum, and $n = 1, 2, 3$. Combining Eqs. (5) and (6) we get the coupled equations for the fluxes through the loops of the SQUIDs in natural units, normalized form as

$$\begin{bmatrix} \ddot{\phi}_1 + \gamma\dot{\phi}_1 + \beta\sin(2\pi\phi_1) \\ \ddot{\phi}_2 + \gamma\dot{\phi}_2 + \beta\sin(2\pi\phi_2) \\ \ddot{\phi}_3 + \gamma\dot{\phi}_3 + \beta\sin(2\pi\phi_3) \end{bmatrix} = \frac{1}{\det(\Lambda)} \begin{bmatrix} 1-\lambda^2 & -\lambda+\frac{\lambda^2}{8} & \lambda^2-\frac{\lambda}{8} \\ -\lambda+\frac{\lambda^2}{8} & 1-\frac{\lambda^2}{64} & -\lambda+\frac{\lambda^2}{8} \\ \lambda^2-\frac{\lambda}{8} & -\lambda+\frac{\lambda^2}{8} & 1-\lambda^2 \end{bmatrix} \begin{bmatrix} \Phi_{ext}-\phi_1 \\ \Phi_{ext}-\phi_2 \\ \Phi_{ext}-\phi_3 \end{bmatrix} \tag{7}$$

,

* jonialdshena@misis.ru

where

$$\Phi_{ext} = \phi_{dc} + \phi_{ac}\cos(\Omega\tau) \qquad (8)$$

end

$$\det(\Lambda) = 1 - \frac{129\lambda^2}{64} + \frac{\lambda^3}{4} \qquad (9)$$

All the fluxes Φ_1, Φ_2, Φ_3, Φ_{ac}, Φ_{dc} are in units of the flux quantum Φ_0 and the new temporal variable t is defined as $\tau = t\omega_{LC}$ with $\omega_{LC} = \frac{1}{\sqrt{LC}}$ being the inductive-capacitive (LC) SQUID frequency. Note that the normalized driving frequency Ω is in units of ω_{LC} i.e., $\Omega = \frac{\omega}{\omega_{LC}}$. The overdots in Eq. 7 denote differentiation with respect to the normalized temporal variable τ. The rescaled SQUID parameter and the loss coefficient are given respectively by $\beta = \frac{LI_c}{\Phi_0}$ and $\gamma = \frac{1}{R}\sqrt{\frac{L}{C}}$.

In what follows, the external dc flux is set to zero, i.e., $\phi_{dc} = 0$. For obtaining the values of the SQUID-dependent normalized parameters β and γ, we choose $L = 120pH$, $C = 1.1pF$, $R = 500\Omega$, and $I_c = 2.35mA$ for their equivalent lumped-circuit elements. By substituting them into the rescaled SQUID parameters β and γ we get $\beta = 0.1369$ and $\gamma = 0.024$, while the LC or geometrical frequency is $f_{LC} = \omega_{LC}/2\pi = 13.9GHz$. Moreover, all the numerical analysis have been obtained using Julia programming language and the DynamicalSystems package [5]. All the code for this paper can be found in https://github.com/Joniald/Squid_Trimer.

III. CHAOS SYNCHRONIZATION

It is known that for relatively high ϕ_{ac}, the single SQUID exhibits a multistable response which is reflected in its corresponding "snake-like" resonance curve [1], as a function of the driving frequency Ω. When two SQUIDs are coupled positively (i.e., when $\lambda > 0$) they exhibit a hysteretic resonance curve with a bubble connected to it through Neimark-Sacker (torus) bifurcations, along with coexisting chaotic branches in their vicinity and the transition to chaos occurs through a period-doubling cascade of a two-dimensional torus (quasiperiodicity-to-chaos transition) [2].

For three coupled SQUIDs (trimer), considering $\phi_{ac} = 0.02$ and $\lambda = 0.1075$, we calculate the Lyapunov exponents (Fig. 2 (a)). Depending on the three maxima Lyapunov exponents $L_1 > L_2 > L_3$ (the rest are negative) and for $\Omega < 1.230$ starting from the right end of the frequency interval, the largest Lyapunov exponent is zero where the others receive values less than zero, indicating
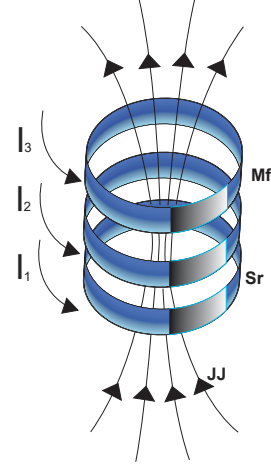

FIG. 1. Schematic diagram of a SQUID trimer with positive magnetic coupling strength, in a magnetic field where (Mf) is the Magnetic field, (Sr) is the Superconducting ring, (JJ) is the Josephson Junction, and (I_1), (I_2) and (I_3) are the induced currents.

a periodic behavior of the system. For $\Omega \geq 1.230$, the presence of two positive Lyapunov exponents confirms that the evolution is hyperchaotic. This is valid up to $\Omega \simeq 1.234$. After this value, hyperchaos no longer exist ($L_1 > 0$ and $L_2 = L_3 \simeq 0$) leading to chaotic motion with some windows in Ω interval where the system is periodic. After $\Omega \geq 1.244$ the evolution ceases to be chaotic. The diagram depicts a transition from chaos to quasiperiodic oscillations through a sequence of period-doubling bifurcations ($L_1 = L_2 = 0$ and L_3 reaches zero for $\Omega \simeq 1.247$).

In order to quantify the synchronization between $\phi_1(t)$ and $\phi_3(t)$ we calculate the η measurement [3]:

$$\eta(t) = \sqrt{(\phi_1(t) - \phi_3(t))^2 + (\dot{\phi_1}(t) - \dot{\phi_3}(t))^2}, \qquad (10)$$

where for η in time close to zero we have almost perfect synchronization. Regarding the η average over time, we have observed, after careful numerical calculations, that the dynamic relationship between $\phi_1(t)$ and $\phi_3(t)$ revels three main behaviors: Synchronization when $\langle\eta\rangle_t < 0.01$ in the interval between $\Omega = 1.223$ and $\Omega = 1.23$, intermittent synchronization when $0.01 < \langle\eta\rangle_t < 0.3$ in the interval between $\Omega = 1.23$ and $\Omega = 1.234$ and no synchronized or unsynchronized solutions when $0.3 < \langle\eta\rangle_t$ in the interval between $\Omega = 1.244$ and $\Omega = 1.2475$ (Fig. 2 (b)). It is remarkable, however, that synchronization can be achieved even in the chaotic regime between $\Omega = 1.234$ and $\Omega = 1.244$ where $L_1 > 0$ and $L_2 = L_3 \simeq 0$, as shown in Fig. 2 (a) . Finally, in Fig. 2 (c) the maxima of the solution for $\phi_1(t)$ is plotted over Ω. For this continuation only one set of different initial conditions were used, however the regions of periodic, hyperchaotic, chaotic and quasiperiodic solutions within the Ω interval are well observed.
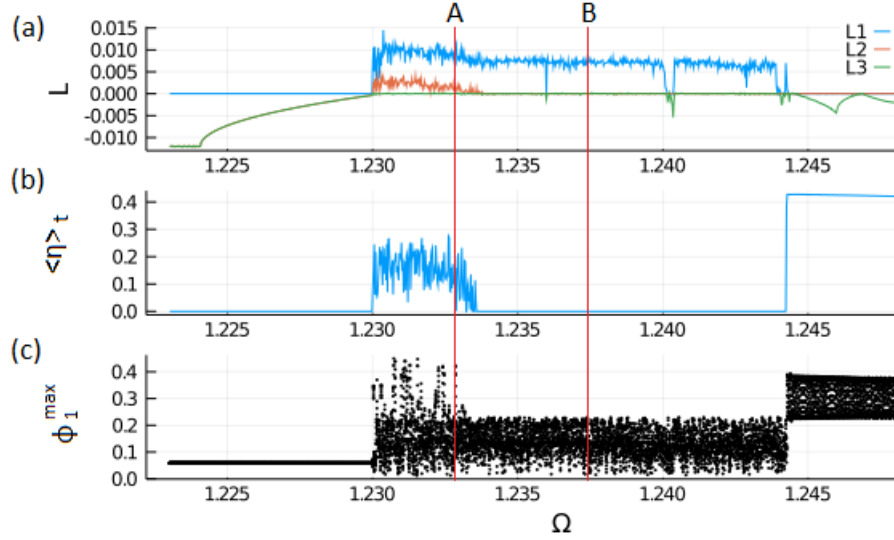
FIG. 2. (a) The three maxima Lyapunov exponents (the rest are negative), (b) the mean value over time of η and (c) maximum value of the magnetic flux ϕ_1 as a function of the driving frequency. Red line A corresponds to $\Omega = 1.233$ and B to $\Omega = 1.2375$. We observe two main regions: The first one is between $(\Omega = 1.23, \Omega = 1.234)$ corresponds to hyperchaos intermittent synchronization where $(\langle\eta\rangle_t < 0.3, L_1 > 0, L_2 > 0, L_3 = 0)$ and the second one lying between $(\Omega = 1.234, \Omega = 1.244)$ corresponds to chaos synchronization where $(\langle\eta\rangle_t \simeq 0, L_1 > 0, L_2 = L_3 = 0)$. Parameters: $\lambda = 0.1075$, $\phi_{ac} = 0.02$, $\gamma = 0.024$, $\phi_{dc} = 0$ and $\beta = 0.1369$.

We examine two main regions in our system by fixing the driving frequency Ω to a certain value. Hyperchaos and chaos have been marked by the red horizontal line A and B (Fig. 2) and the temporal evolution in SQUID 1 and 3 have been plotted for the respective areas ($\Omega = 1.233$ and $\Omega = 1.2375$) as shown in Fig. 3 (a) and (b). Blue represents the first SQUID and red the third SQUID. For $\Omega = 1.233$, the time evolution of ϕ_1 and ϕ_3 are not synchronized (Fig. 3 (a)) although, there are some windows in time where synchronization occurs. This is a hyperchaos intermittent synchronization and we will address this phenomena in more details in the next section. This unsynchronized behavior can be confirmed in both (ϕ_1, ϕ_2) and (ϕ_1, ϕ_3) plane projections (Fig. 3 (c), (e)). Synchronized chaos can be seen in Fig. 3 (b) as the time series of the trimer edges are identical. The projection of the flow onto the (ϕ_1, ϕ_3) plane confirm this behavior (Fig. 3 (f)), in contrast with the (ϕ_1, ϕ_2) plane projection where no synchronization occurs (Fig. 3 (d)).

FIG. 3. Unsynchronized chaos for a set of parameters as in Fig. 2 (A red line) where $\Omega = 1.233$. (a) Time series for ϕ_1 (blue color) and ϕ_3 (red color). (c) Projection of the flow onto ϕ_1 - ϕ_2 plane. (e) Projection into the ϕ_1 - ϕ_3 plane. (b), (d) and (f) the same for synchronized chaos where the set of parameters as in Fig. 2 (B red line) where $\Omega = 1.2375$.

IV. THE PARAMETER SPACE

As we mentioned early, for the η average over time, we observe three main behaviors: Synchronization, intermittent synchronization and no synchronized or unsynchronized solutions. Moreover, by calculating the Lyapunov exponents we have periodic solutions, quasiperiodicity, chaos and hyperchaos. In Fig.4, a map of different dynamic regions in combination with $\langle\eta\rangle_t$ and maxima Lyapunov exponents are shown in (Ω, λ) (Fig.4 (a)) and (Ω, ϕ_{ac}) (Fig.4 (b)) parameter space. We ob-
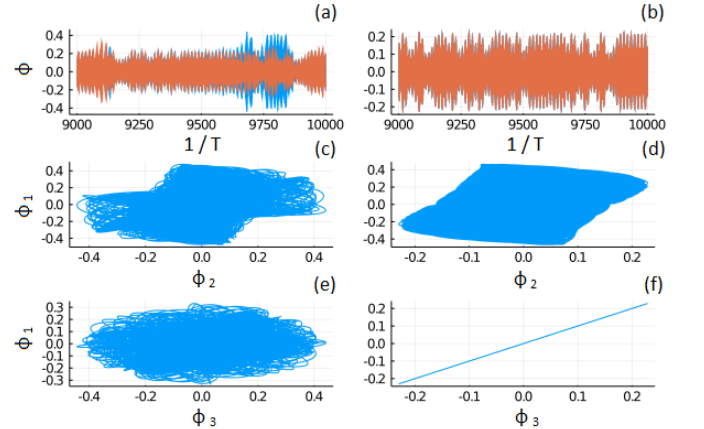
serve six different areas. Periodic synchronization (PS) where $L_1 = 0, L_2, L_3 < 0$ and $\langle\eta\rangle_t < 0.01$, periodic unsynchronized solution (PUn) where $L_1 = 0, L_2, L_3 < 0$ and $0.3 < \langle\eta\rangle_t$, quasiperiodic unsynchronized solution (QPUn) where $L_1 = L_2 = 0, L_3 < 0$ and $\langle\eta\rangle_t > 0.3$, chaos synchronization (CS) where $L_1 > 0, L_2 = L_3 = 0$ and $\langle\eta\rangle_t < 0.01$, chaos intermittent synchronization (CI) where $L_1 > 0, L_2 = L_3 = 0$ and $0.01 < \langle\eta\rangle_t < 0.3$ and finally hyperchaos intermittent synchronization (HCI)
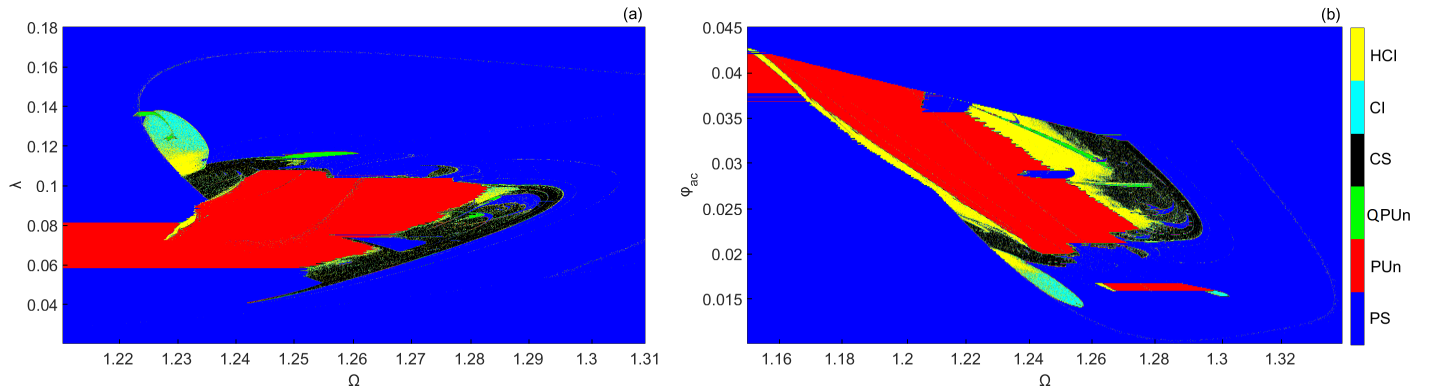
FIG. 4. Map of different dynamical regions in the (a) (λ,Ω) parameter space where $\phi_{ac} = 0.02$ and (b) in the (ϕ_{ac},Ω) parameter space where $\lambda = 0.02$. Depending on three maxima Lyapunov exponents ($L_1 > L_2 > L_3$) and $\langle \eta \rangle_t$ quantifier, we observe six different areas. Periodic synchronization (PS), Periodic Unsynchronized solutions (PUn), Quasiperiodic unsynchronized solution (QPUn), Chaos synchronization (CS), Chaos intermittent synchronization (CI) and finally Hyperchaos intermittent synchronization (HCI). Other parameters: $\gamma = 0.024$, $\phi_{dc} = 0$ and $\beta = 0.1369$.

where $L_1 > 0, L_2 > 0, L_3 = 0$ and $0.01 < \langle \eta \rangle_t < 0.3$.

Both in the parameter interval (Ω,λ) and (Ω,ϕ_{ac}), periodic synchronization (PS) occupies most of the surface. Next, the main dynamic behavior is concentrated in a periodic unsynchronized solution (PUn). At the boundaries of this region, we observe chaos synchronization (CS) and hyperchaos intermittent synchronization (HCI). It is remarkable that hyperchaos always appears with intermittent synchronization of $\phi_1(t)$ and $\phi_3(t)$. We have never observed synchronization or unsynchronized solutions between the trimer edges, in the presence of hyperchaos. The opposite is not true. Indeed, intermittent synchronization can also be observed in the chaotic regime (Fig.4, Maya blue color (CI)). Finally, very small areas of quasiperiodic unsynchronized solutions (QPUn) fill the parameter space.

Three specific dynamic regions of non chaotic behavior are shown in Fig. 5 with constant $\phi_{ac} = 0.02$. The time series of the magnetic flux (Fig. 5 (a) first column), for $\Omega = 1.21$ and $\lambda = 0.16$, show a periodic synchronization between the first (red color) and third (blue color) SQUID. The time series of η close to zero also indicate a synchronization behavior (Fig. 5 (a) second column). When $\Omega = 1.24$ and $\lambda = 0.07$, $\phi_1(t)$ and $\phi_3(t)$ oscillate out of phase, with different amplitudes, where η also oscillate over time with an average time value greater than 0.3, an indication for a periodic unsynchronous solution (Fig. 5 (b) first and second column). For $\Omega = 1.255$ and $\lambda = 0.118$, the temporal evolution of the system is quasiperiodic and the magnetic flux of the first and third SQUIDs oscillates in time with different frequencies and amplitudes (Fig. 5 (c) first column). The η quantifier also has a period evolution with multiple frequencies due to the quasiperiodic behavior, where $0.3 < \langle \eta \rangle_t$ as an evident of non-synchronization between the trimer edges.

Figure. 6 illustrates three other dynamic examples, this time in the chaotic regime. For $\Omega = 1.235$ and $\lambda = 0.1$ the temporal evolution of the system is chaotic and the output magnetic fluxes in SQUID 1 and 3 are identical, as shown in Fig. 6 (a), first column. This chaotic synchronization is confirmed by the evolution of η close to zero in the second column. When $\Omega = 1.23$ and $\lambda = 0.125$ the time series of the trimer edges are chaotic but not identical. The three maxima Lyapunov exponents associated with this evolution are $(+0.007, -3.3e-5, +1.7e-5)$. Nevertheless, there are some windows in time where synchronization occurs (Fig. 6 (b), first column). This is a chaos intermittent synchronization where η evolves, at some temporal intervals close to zero (synchronous behavior) and at others with large fluctuations between zero and one (Fig. 6 (b), second column). The same dynamic behavior as the previous is demonstrated in Fig. 6 (c) for both $\phi_1(t)$ and $\phi_3(t)$ (first column) and η quantifier (second column) where $\Omega = 1.23$ and $\lambda = 0.11$. However, in this case, the associated three maxima Lyapunov exponents are $(+0.015, +0.002, -6.7e-6)$. The system is now hyperchaotic, with more than one positive Lyapunov exponent and so the behavior of the system is characterized as hyperchaotic intermittent synchronization.
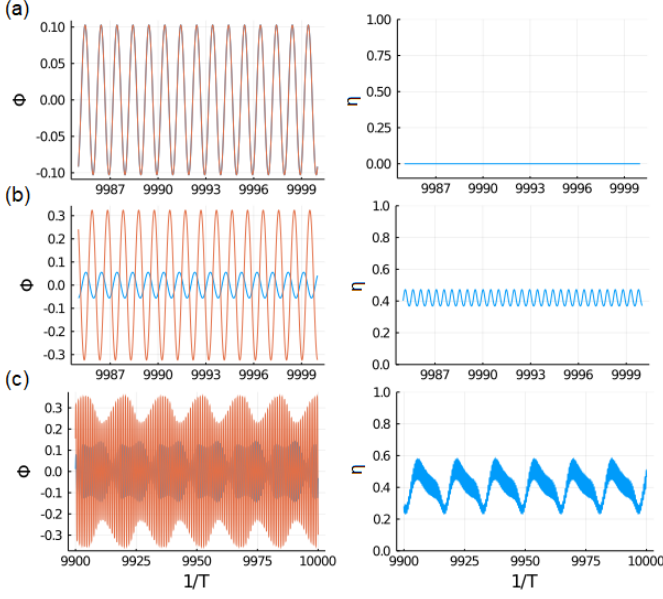
V. CONCLUSIONS

VI. ACKNOWLEDGEMENTS

FIG. 5. (a) Periodic synchronization (PS) where $\Omega = 1.21$ and $\lambda = 0.16$. (b) Periodic unsynchronized (PUn) solution where $\Omega = 1.24$ and $\lambda = 0.07$ (c) Quasiperiodic unsynchronized (QPUn) solution where $\Omega = 1.255$ and $\lambda = 0.118$. In first column the time series of the magnetic flux for the first SQUID, (red line), and the third SQUID, (blue line). In second column η over time. Other parameters: $\phi_{ac} = 0.02$, $\gamma = 0.024$, $\phi_{dc} = 0$ and $\beta = 0.1369$.
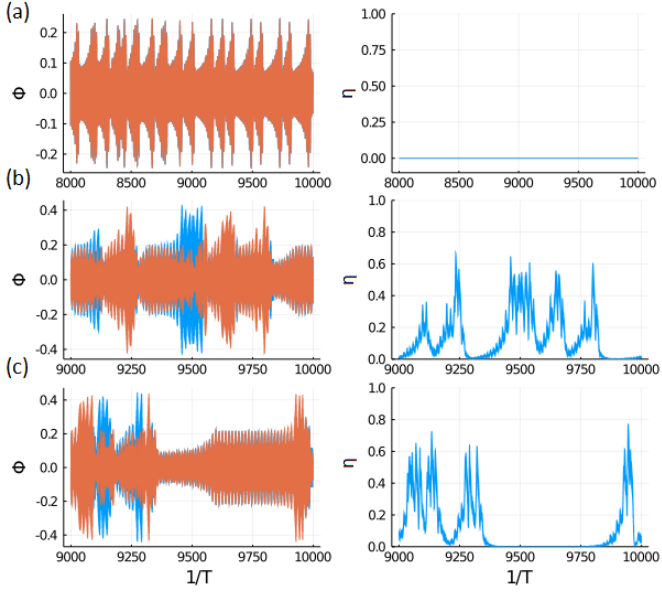

FIG. 6. (a) Chaos synchronization (CS) where $\Omega = 1.235$ and $\lambda = 0.1$. (b) Chaos intermittent synchronization (CI) where $\Omega = 1.23$ and $\lambda = 0.125$. (c) Hyperchaos intermittent synchronization (HCI) where $\Omega = 1.23$ and $\lambda = 0.11$. First and second column as in Fig.5. Other parameters: $\phi_{ac} = 0.02$, $\gamma = 0.024$, $\phi_{dc} = 0$ and $\beta = 0.1369$.

[1] J. Hizanidis, N. Lazarides, and G. P. Tsironis, Chaos: An Interdisciplinary Journal of Nonlinear Science **28**, 063117 (2018), https://doi.org/10.1063/1.5020949.

[2] J. Shena, N. Lazarides, and J. Hizanidis, Chaos: An Interdisciplinary Journal of Nonlinear Science **30**, 123127 (2020), https://doi.org/10.1063/5.0018362.

[3] G. L. Baker, J. A. Blackburn, and H. J. T. Smith, Phys. Rev. Lett. **81**, 554 (1998).

[4] H. G. Winful and L. Rahman, Phys. Rev. Lett. **65**, 1575 (1990).

[5] G. Datseris, Journal of Open Source Software **3**, 598 (2018).